High Enzymatic Activity Preservation with Carbon Nanotubes Incorporated in Urease-Lipid Hybrid Langmuir-Blodgett Films

ARTICLE *in* LANGMUIR · FEBRUARY 2012

Impact Factor: 4.46 · DOI: 10.1021/la300193m · Source: PubMed

2 AUTHORS:

Luciano Caseli
Universidade Federal de São Paulo
81 PUBLICATIONS **1,196** CITATIONS
SEE PROFILE

José Roberto Siqueira Jr.
Universidade Federal do Triangulo Mineiro (U…
25 PUBLICATIONS **530** CITATIONS
SEE PROFILE

Langmuir

Article

pubs.acs.org/Langmuir

High Enzymatic Activity Preservation with Carbon Nanotubes Incorporated in Urease–Lipid Hybrid Langmuir–Blodgett Films

Luciano Caseli*,† and José Roberto Siqueira, Jr.*,‡

†Instituto de Ciências Ambientais, Químicas e Farmacêuticas, Universidade Federal de São Paulo (UNIFESP), Diadema, São Paulo (SP) 09972-270, Brazil

‡Instituto de Ciências Exatas, Naturais e Educação, Universidade Federal do Triângulo Mineiro (UFTM), Uberaba, Minas Gerais (MG) 38025-180, Brazil

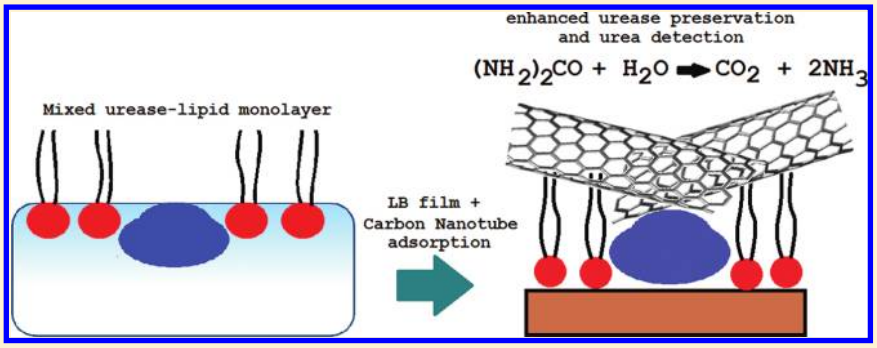

ABSTRACT: The search for optimized architectures, such as thin films, for the production of biosensors has been challenged in recent decades, and thus, the understanding of molecular interactions that occur at interfaces is essential to improve the construction of nanostructured devices. In this study, we investigated the possibility of using carbon nanotubes in hybrid Langmuir–Blodgett (LB) films of lipids and urease to improve the catalytic performance of the immobilized enzyme. The molecular interactions were first investigated at the air–water interface with the enzyme adsorbed from the aqueous subphase onto Langmuir monolayers of dimyristoylphosphatidic acid (DMPA). The transfer to solid supports as LB films and the subsequent incorporation of carbon nanotubes in the hybrid film permitted us to evaluate how these nanomaterials changed the physical properties of the ultrathin film. Colorimetric measurments indicated that the presence of nanotubes preserved and enhanced the enzyme activity of the film, even after 1 month. These results show that the use of such hybrid films is promising for the development of biosensors with an optimized performance.

1. INTRODUCTION

The immobilization of enzymes in lipid hybrid Langmuir–Blodgett (LB) films is a well-established methodology to preserve the structure of polypeptides in the mild environment provided by the lipids.[1,2] The conservation of the enzyme structure and consequent maintenance of its catalytic activity is important in nanobiotechnology in the sense that the hybrid films may be employed as sensors and other electronic and optical devices. In recent years, several examples of enzyme–lipid hybrid Langmuir and LB films have been reported, including alkaline phosphate,[3] acetylcolinesterase,[4] alcohol dehydrogenase,[5] horseradish peroxidase,[6] catalase,[7] phospholipases,[8] and others.[9,10] Particularly, urease, important in biomedicine, such as, for instance, to remediate urinary pathogens, is an enzyme responsible for the hydrolytic catalysis of urea. In this sense, the production of urea sensors has been recently reviewed,[11] showing the recent developments and different strategies for constructing biosensors as well as showing the analytical performance of each sensor. Urease has recently been investigated at the air–water interface[12] and immobilized in solid supports as a LB film.[13] In a recent paper,[14] it was shown that urease can be immobilized in a negative-charged phospholipid LB film, adopting a closely packed arrangement, which hindered the charge transport across the film and preserved the enzyme activity. Additionally, the ultrathin film could be employed to detect urea with colorimetry.

In particular, the employment of a chemical component may facilitate the transport of charge involved in urea hydrolysis, whose reaction results in the formation of ammonium, altering the protonation of the medium. In this context, carbon nanotubes (CNTs) have been described in the literature as an able material to facilitate charge-transfer reactions and also to interfere in the conformation of hybrid films.[15−20] The advantage of using CNTs rises from their biocompatibility, permitting the immobilization of biomolecules with their biological activity preserved, in addition to the enhanced electronic properties that allow for direct charge transfer between proteins and electrode surfaces. Concerning the formation of hybrid films, CNTs are advantageous, because

Received: January 13, 2012
Revised: February 16, 2012
Published: February 29, 2012

   dx.doi.org/10.1021/la300193m | *Langmuir* 2012, 28, 5398–5403

they lead to the formation of a porous nanostructure with a large surface area that may contribute to a better electrode–electrolyte interface. These properties are important to obtain sensing units with higher sensitivity for specific and selective detection.[21−27]

In this paper, we present for the first time the introduction of CNTs in urease–lipid hybrid LB films. The influence of CNT incorporation over the surface chemistry of the films and their interactions are discussed, as well as the consequences and advantages in terms of enzyme activity preservation.

2. MATERIALS AND METHODS

2.1. Materials. Dimyristoylphosphatidic acid (DMPA, Sigma-Aldrich) and urease from jack beans (29 500 units/g, Sigma), NaCl (99%), sodium phosphate monobasic (98%), ethylenediaminetetraacetic acid (EDTA), and sodium 4 phosphate dibasic (99%) were purchased from Merck. This lipid was chosen because of the regular pattern of deposition as a LB film, as already reported in previous papers.[28] Bromocresol purple was obtained from Sigma-Aldrich. Water was supplied by a Milli-Q system (resistivity = 18.2 MΩ cm at 23 °C and pH 6.3). All other reagents were of the highest purity commercially available.

2.2. Langmuir Monolayer Preparation. The Langmuir monolayers were prepared on a mini-KSV Langmuir trough (system 2, total volume of 220 mL), equipped with a Wilhelmy plate made of a filter paper and a Kelvin probe to measure the surface potential. Langmuir monolayers of DMPA were obtained by spreading a chloroform [Sigma, high-performance liquid chromatography (HPLC) grade]/methanol (Sigma, HPLC grade) solution (9:1, mol/mol) of the lipid on the surface of the aqueous subphase, made of 0.1 mol L^{-1} phosphate buffer (pH ∼ 7.2) and 0.1 mol L^{-1} NaCl.

Aliquots of 25 μL of a 25 mg mL^{-1} urease solution (prepared in a 0.1 mol L^{-1} phosphate buffer at pH ∼ 7.2) were injected in the subphase after DMPA spreading a few millimeters below the air–water interface. For the subphase volume of 220 mL, the final enzyme concentration was 2.8 mg L^{-1}. After injecting the urease solution and the stabilization of surface pressure, the monolayer was then compressed.

2.3. Langmuir Monolayer Characterization. Surface pressure–area (π–A) isotherms were obtained with a monolayer compression rate of 0.5 $Å^2$ $molecule^{-1}$ min^{-1}, with the subphase at 23 ± 1 °C. DMPA was compressed after surface pressure stabilization, which usually took ca. 1 h.

Polarization–modulation infrared reflection absorption spectroscopy (PM-IRRAS) measurements were carried out with a KSV PMI 550 instrument (KSV Instrument, Ltd., Helsinki, Finland). The Langmuir trough was set up so that the light beam reaches the monolayer at a fixed incidence angle of 75°. The incoming light is continuously modulated between s and p polarization at a high frequency, which allows for the simultaneous measurement of the spectra for the two polarizations. The difference between the spectra provides surface-specific information, and the sum provides the reference spectrum. With the simultaneous measurements, the effect of the water vapor is largely reduced. The resolution of the spectra is of 5 cm^{-1}.

2.4. LB Films. The transfer of DMPA monolayers and urease–DMPA hybrid monolayers onto different solid supports (see below) was performed at a surface pressure of 30 mN m^{-1}. The monolayer was kept at this pressure for 20 min to guarantee stability, after which the solid support, already immersed in the subphase, was taken off from the subphase. The dipping speed was 2.0 mm min^{-1}, and the transfer ratio (always close to 1.0) served as a first parameter of quality. In additional experiments, urease–DMPA hybrid films were inserted in CNT [single-walled polyaminobenzene sulfonic acid functionalized (Sigma-Aldrich)] suspensions (0.5 mg/mL in water) for 10 min and washed with water. Also, pure DMPA LB films were dipped in a urease solution (2.8 mg L^{-1}) for 10 min.

Additional experiments were performed by dipping the film formed with urease adsorbing from solution on the preformed DMPA LB film in the CNT suspension, forming a three-layer layer-by-layer (LbL) film [(i) DMPA + (ii) urease (from solution) + (iii) CNT (from suspention)].

The formation of LB and LbL films was confirmed with PM-IRRAS and nanogravimetry analyses with a quartz crystal microbalance (QCM, Stanford Research Systems, Inc.) to evaluate the mass transferred. For PM-IRRAS, we employed quartz as a solid support, and for QCM, we used AT-cut quartz crystals, coated with Au (Stanford Research Systems, Inc.) with a fundamental frequency of ca. 5 MHz. The morphology of the films were investigated by atomic force microscopy (AFM) images, using a digital AFM nanoscope IIIA instrument with a silicon tip in the contact mode and employing a resonance frequency of approximately 300 kHz and a scan rate of 1.0 Hz. For that, the films were deposited on silicon plates.

To investigate the activity of free and immobilized urease, we monitored the time dependence of the optical absorbance at 588 nm after introducing urease in a solution with bromocresol purple according to the method described in the literature.[14] A solution containing adjustable concentrations of urea, 0.015 mmol L^{-1} bromocresol purple, and 0.2 mmol L^{-1} EDTA was adjusted to pH 5.8 with diluted NaOH aqueous solution. Then, we introduced the urease-containing films into the bromocresol solution. The hydrolysis of urease produced ammonia, thus increasing the pH and enhancing the absorbance of the pH-sensitive dye (bromocresol purple). The enzyme activity was estimated from the rate of ammonium production with time.

3. RESULTS AND DISCUSSION

3.1. Air–Water Interface. The incorporation of urease in Langmuir monolayers was first investigated with surface pressure–area isotherms. In Figure 1, we observe that the curve is shifted to larger areas, which can be related to the adsorption of the enzyme after 1 h of its injection below the DMPA monolayer. Although no significant increase of the surface pressure could be observed at large molecular areas for DMPA, the differences between the two curves at lower molecular areas are evident. Even at surface pressures close to the collapse, we note the shift of the curve for the hybrid monolayer to higher areas. For instance, in the surface pressure of 30 mN/m, the molecular area for DMPA is shifted from 38.5 to 43.0 $Å^2$. This increase in the molecular area could be roughly attributed to the occupancy of urease in the surface pressure of 30 mN/m. In this way, considering the approximate molecular ratio of 175:1 of lipid/enzyme, this difference of 4.5 $Å^2$ in the molecular area for DMPA would correspond to a molecular

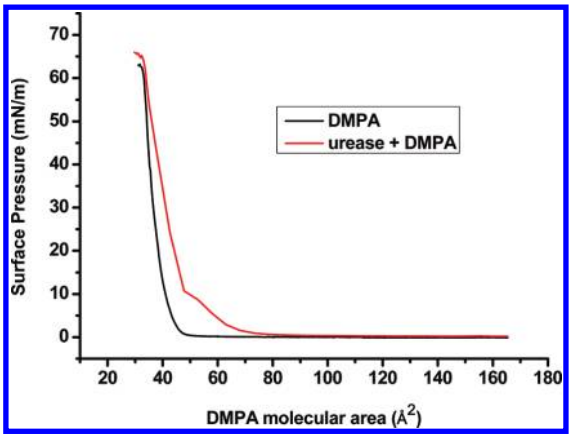

Figure 1. Surface pressure–area isotherm for DMPA monolayers, pure or interacting with urease in the subphase (2.8 mg/L).

dx.doi.org/10.1021/la300193m | Langmuir 2012, 28, 5398−5403

occupancy for urease of 175 times greater, i.e., 2250 Å^2, which is close to the molecular dimensions of this protein.[28]

This is the first evidence that a great amount of protein was incorporated in the interface. Only at surface pressures as high as 60 mN/m, the π−A curves for both monolayers are practically coincident. In this case, the proximity to the 2D−3D transition could lead to the expulsion of the protein.[29] Also, we observe for the hybrid film isotherm a plateau around 8−10 mN/m, which is generally observed, according to the literature, for DMPA monolayers in certain conditions of temperature and pH.[28,30,31] This indicates that the presence of urease induces a first-order transition for the monolayer, going from a liquid-expanded phase to a liquid-condensed phase. Because CNTs were incorporated in the LB films and not in the Langmuir monolayer, it is likely that the phase transition on the urease−DMPA Langmuir monolayer would not affect the further CNT incorporation. The incorporation of urease in such small quantities did not separate phases, as attested in previous experiments in our group.

Also, the surface pressure of collapse for the hybrid monolayer (66 mN/m) is close to the value obtained for the pure DMPA monolayer (around 64 mN/m), showing that the presence of the protein keeps the monolayer as resistant to compression as that for the pure DMPA monolayer.

Such changes in the organization of the monolayer could be better investigated in Figure 2A, in which the infrared spectra in the C−H region show slight changes in the band positions as long as the monolayer compression is carried out. The band in 2920 cm^{-1}, attributed to C−H antisymmetric stretches in CH_2, is shifted to lower energies with the introduction of urease. On the other hand, the band 2881 cm^{-1}, attributed to C−H stretches in CH_3, practically disappears with the incorporation of urease at low lipid molecular areas. With the monolayer compressed to the surface pressure of 30 mN/m, this band is shifted to higher energies. The intensity of the band in 2837 cm^{-1}, attributed to symmetric stretches in CH_2, becomes relatively higher with urease incorporation. The relation between the integrated areas below the bands for CH_3 and antisymmetric CH_2 stretches changed from 1.8 for pure DMPA to 0.7 for urease−DMPA (0 mN/m) and to 0.8 when the mixed monolayer was compressed to 30 mN/m. This relation could be attributed to an order parameter.[32] These values corroborate the fact that the presence of urease decreases the order of the packed structure resulted from a pure DMPA monolayer.

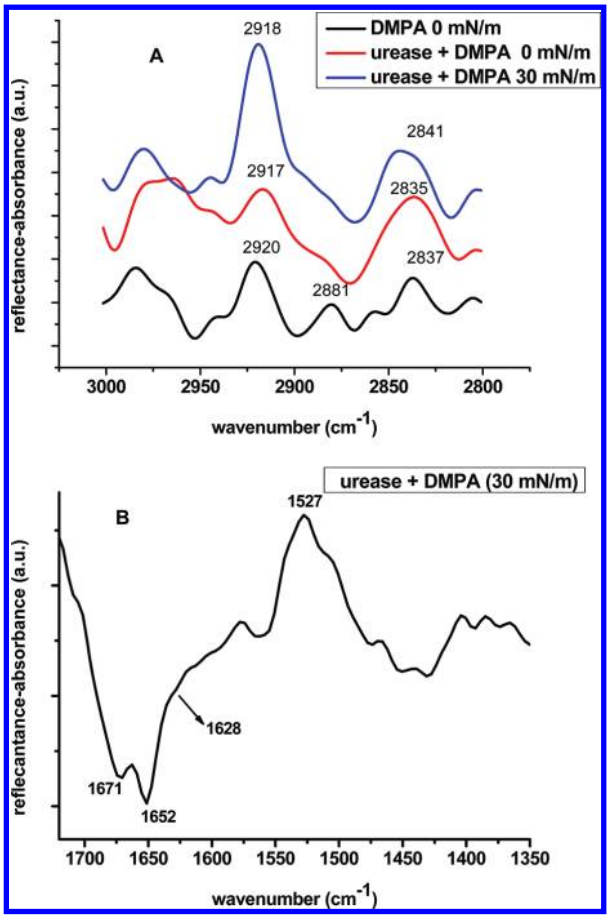

Figure 2. PM-IRRAS spectra for DMPA (pure or hybrid with urease in the subphase at 2.8 mg/L). Panel A shows the range for C−H stretches. Panel B shows the range for amide I and II vibrations.

Figure 2B shows the presence of amide bands, confirming the incorporation of the enzyme at the interface. Because basically the spectrum does not change from 0 to 30 mN/m, we show only the spectrum for 30 mN/m. The amide I bands are negative, indicating that C═O vibrational transition dipoles are mainly perpendicular to the interface normal. The band in 1652 cm^{-1} indicates the predominance of α-helix structures,[33] and the band in 1671 cm^{-1} is attributed to disordered chains or β-turns.[33] This band could also be associated to O−H bending of interfacial water, as a result of the difference between the water surface covered with the monolayer and the water surface directly exposed to the air phase.[34] Contribution of β-sheet structures is defined by a shoulder at 1628 cm^{-1}, proving the predominance of α-helices. This is in agreement with the polypeptide structure determined using X-ray crystallography.[35] The band at 1527 cm^{-1} is called the amide II band (C−N stretch or N−H bend). Because the spectra did not change significantly with those spectra for the pure enzyme,[36] it can be concluded that the presence of DMPA maintains the structure of the enzyme little affected.

3.2. Deposition on Solid Supports. After transferring the pure or hybrid DMPA monolayer to the solid supports at a surface pressure of 30 mN/m, the quality of deposition was first analyzed through the transfer ratios, which were close to unity. Then, we incorporated CNTs by dipping the LB film into a suspension that contained CNTs. Figure 3 shows that, when we have only one layer of a urease−DMPA hybrid film, wide bands are obtained and also the amide I bands (1600−1700 cm^{-1}) are not clearly defined. With CNT incorporation, the bands become more defined, with an amide I band in 1657 cm^{-1}, indicating α-helices, and the other band in 1632 cm^{-1}, indicating that some β-sheets are appearing because of the interaction with CNTs. However, it is important to emphasize that this band is owing to an effect of the molecular reaccommodation of the own protein as a result of noncovalent CNT−protein interactions and not from the CNTs because it does not present chemical groups that should interacts specifically with the amide regions. For the monolayer at the air−water interface, a β-sheet band appeared as a shoulder in low energies. A similar behavior is observed for a film produced with DMPA LB dipped in the urease solution followed by dipping it into the CNT suspension, as described in the Materials and Methods. Again, the amide I band becomes more defined, with a β-sheet band appearing in 1625 cm^{-1}. The band in 1644 cm^{-1} indicates non-ordered structures of the enzyme.

dx.doi.org/10.1021/la300193m | Langmuir 2012, 28, 5398−5403

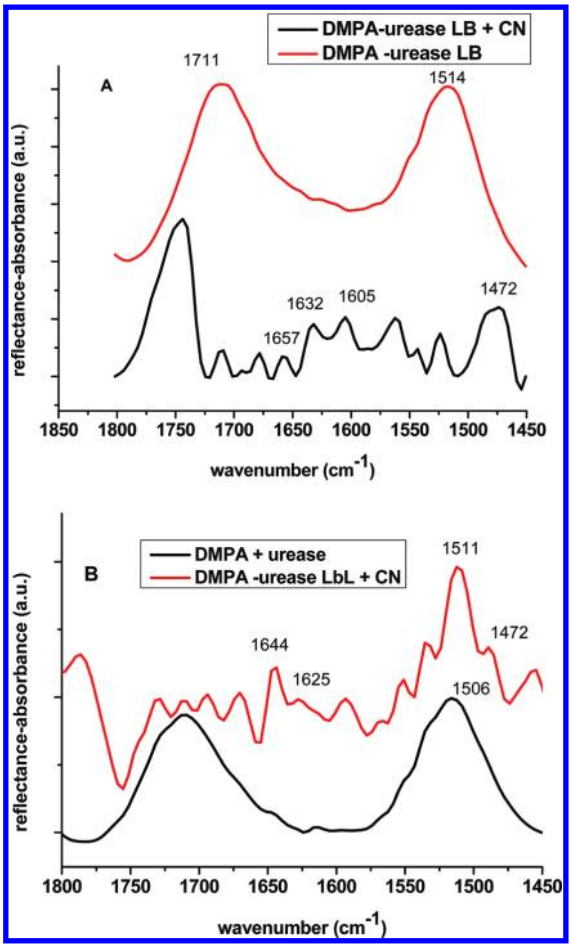

Figure 3. PM-IRRAS spectra for the urease−DMPA hybrid ultrathin film with or without CNT adsorbed from its suspension. Panel A shows the enzyme−lipid hybrid film produced from the LB technique. Panel B shows the enzyme−lipid hybrid film produced from adsorption of urease from solution of a preformed DMPA LB film.

This means that probably the α-helice structure is lost in the LbL film. Also, the amide II band is more intense than the amide I band, which is another indication that the enzyme lost its native secondary structure significantly.[37] Also, for both films, a band in 1472 cm^{-1} appears after CNT incorporation. This band can be attributed to C−H bends present in the alkyl structure of DMPA. These results therefore show that the CNTs interact with both kinds of compounds present in the hybrid films: lipids and proteins. It is likely that these interactions are of a noncovalent nature (van der Waals forces) and may involve contact of CNTs with DMPA. Probably urease molecules may not completely cover the layer of DMPA and also that the CNTs can interpenetrate in the protein layer, interacting with the lipid adsorbed directly on the solid support.

To analyze the morphology of the different films formed, we obtained AFM images for a scanned area of 1.0 μm^2, as shown in Figure 4. All of the films are relatively homogeneous with little points of heterogeneity, indicating the CNTs were probably embedded into the lipid−protein structure, stabilizing the film. A higher resolution for the AFM images was also shown (until 0.1 × 0.1 μm) to obtain details on the CNT structures, but no better elements could be observed. Probably the three-component mixture resulted in a highly homogeneous film that did not enable us to obtain images, allowing for the specific location of the CNTs. This is another indication that the CNTs interpenetrated into the protein−lipid molecular structure, leading to a more homogeneous pattern for the films.

For the pure DMPA LB film (panel A), we note a flat pattern, as expected.[38] For urease−DMPA hybrid LB film (panel B), the heterogeneity in some points suggests the incorporation of the enzyme. This heterogeneity increases for the film as shown in panel C, indicating the effect of the subsequent adsorption of CNT. When the enzyme was incorporated from its solution in the pure DMPA LB film (panel D), we observe some points of heterogeneity distributed more irregularly than the image shown in panel B. However, the adsorption of CNT onto this film (panel E) causes the points to be more distributed, increasing the heterogeneity of the film and also leading to the appearance of a valley as a defect. These defects in the films not only indicate the enzyme and CNT adsorption but also can result in important consequences in the chemical or biological function of these materials. For that, we investigate the enzyme activity of urease in the different architectures for the films produced and compare to the enzyme activity in homogeneous solution, with the same amount of enzyme, estimated using the QCM. In other words, we investigated if these films are able to detect analytical quantities of urea.

As a result, we can observe in Table 1 that the incorporation of CNT in urease−DMPA film for both kinds of film causes the increase of the enzyme activity. Also, CNT-containing films had the least loss of enzyme activity after 1 month. Particularly, for the LB film, we have obtained the best catalytic activity and also stability.

The same outcome could be obtained when we use other urea concentrations. Also, these results can be better evaluated with the Michaelis−Menten parameters obtained for urea concentrations ranging from 0.1 to 5 μM (Table 2). This means, in short, that an analytical curve could be obtained in this range and the enzyme presents Michaelis−Menten kinetics behavior.

Consequently, the presence of CNT enhanced some properties of the film, as also reported for other kinds of nanostructures.[22−27,39] In these works, different types of nanoarchitectures made of CNT with polyamidoamine (PAMAM) dendrimers combined with specific compounds were studied to detect dopamine and ascorbic acid,[22] penicillin,[24,25] and hydrogen peroxidase.[39] In our specific case, the interaction of CNTs with the enzyme allowed it to be better positioned into the packed DMPA LB film, conserving better its secondary structures and thus permitting a minimum loss of catalytic activity. It is known that the porous nanostructure of CNTs could be formed with a large surface area, but this may be not the case in the present work. The CNTs are connected with proteins, and results in the enhancement of the enzyme activity are due to fact that the films become more stable in the sense that the way by which the film were constructed led to a better molecular accommodation of the enzyme, facilitating the access of the catalytic substrate.

Finally, it can be concluded that the use of mixed CNT−urease−phospholipid LB films are particularly remarkable because the enzyme is incorporated in a highly organized system, affecting the films ability to detect urea. Although as far as the sensing ability is concerned, further work is required to optimize the biosensor performance.

dx.doi.org/10.1021/la300193m | *Langmuir* 2012, 28, 5398−5403

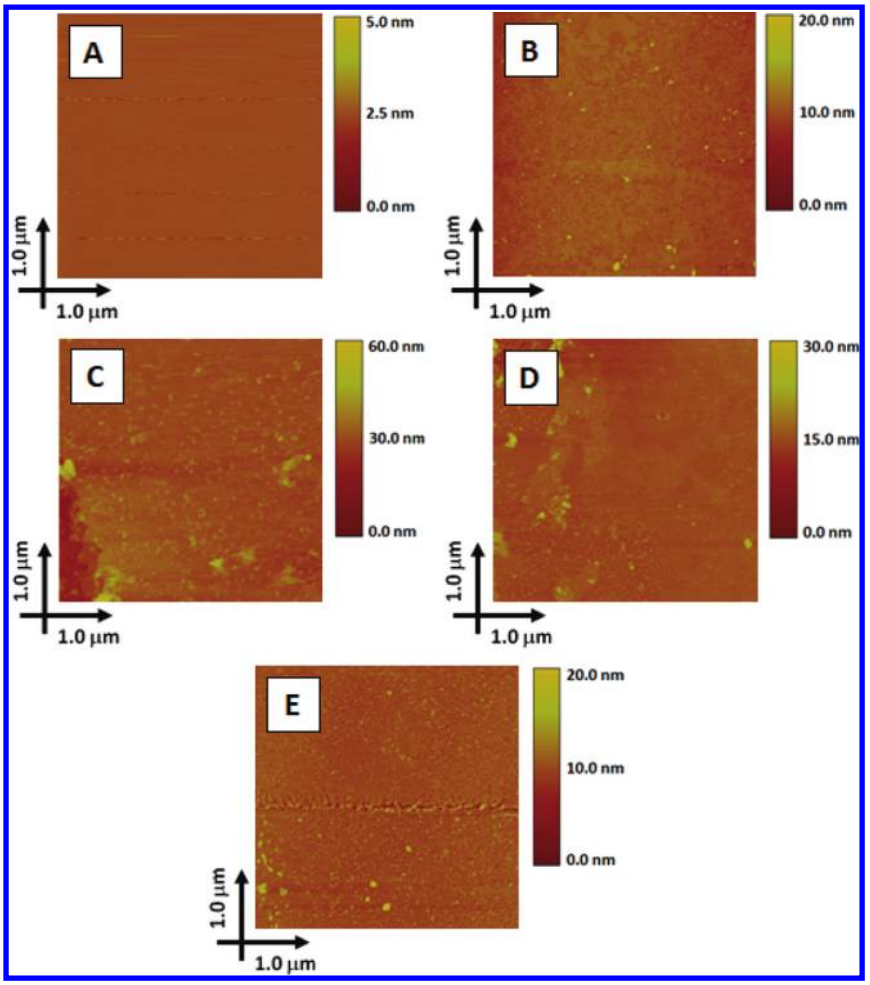

Figure 4. AFM micrographs for (A) pure DMPA LB film, (B) DMPA–urease hybrid LB film, (C) CNTs incorporated on DMPA–urease hybrid LB film, (D) urease incorporated on pure DMPA LB film, and (E) CNTs incorporated on urease incorporated on pure DMPA LB film.

Table 1. Enzyme Activity in 1 μM Urea

	activity to the homogeneous solution (%)	activity (after 1 week) (%)	loss of activity (1 week) (%)	loss of activity (1 month) (%)
urease–DMPA LB film	23	1	96	100
urease adsorbed from solution on DMPA LB film	15	less than 1	~100	100
CNT + urease–DMPA LB film	45	40	11	23
CNT + urease adsorbed from solution on DMPA LB film	27	24	11	20

Table 2. Michaelis–Menten Parameters for Urease–DMPA Hybrid Films

	activity to the homogeneous solution (%)	K_m (mmol/L)	V_{max} (μmol L^{-1} min^{-1})
homogeneous solution	100	43.2	1.98
urease–DMPA LB film	25 ± 7	10.8	4.05
urease adsorbed from solution on DMPA LB film	13 ± 5	5.6	4.88
CNT + urease–DMPA LB film	47 ± 2	20.3	2.88
CNT + urease adsorbed from solution on DMPA LB film	27 ± 2	11.7	2.78

4. CONCLUSION

In summary, this study was aimed at providing a proof-of-concept experiment, to fabricate a urease–DMPA hybrid LB film combined with CNTs. The CNT incorporation significantly modified the chemical structures of the film compounds as demonstrated by the infrared analysis, being confirmed by changes in the film morphology as shown in AFM images. The structure of DMPA–CNT created an appropriate environment to preserve the enzymatic activity of urease into the LB film even after 1 month, leading to films with an enhanced performance and a good sensitivity to detect urea. These results may envisage the feasibility of using such structures as sensing units to develop a urea biosensor for biomedical application.

AUTHOR INFORMATION

Corresponding Author

*E-mail: lcaseli@unifesp.br (L.C.); jr.siqueira@fisica.uftm.edu.br (J.R.S.).

Notes

The authors declare no competing financial interest.

■ ACKNOWLEDGMENTS

The authors are grateful to CNPq, FAPESP, and Rede Nanobionet, Films and Sensors (CAPES, Brazil) for the financial support and the "Laboratório de Filmes Finos" from IFUSP for performing the AFM images.

■ REFERENCES

(1) Girard-Egrot, A. P.; Godoy, S.; Blum, L. J. *Adv. Colloid Interface Sci.* **2005**, *116*, 205−225.
(2) Iost, R. M.; Madurro, J. M.; Brito-Madurro, A. G.; Nantes, I. L.; Caseli, L.; Crespilho, F. N. *Int. J. Electrochem. Sci.* **2011**, *5*, 1085−1104.
(3) Caseli, L.; Masui, D. C.; Prazeres, R.; Furriel, M.; Leone, F. A.; Zaniquelli, M. E. D. *Thin Solid Films* **2007**, *515*, 4801−4807.
(4) Choi, J. M.; Kim, Y. K.; Lee, I. H.; Min, J. H.; Lee, W. H. *Biosens. Bioelectron.* **2001**, *16*, 937−943.
(5) Caseli, L.; Perinotto, A. C.; Viitala, T.; Zucolotto, V.; Oliveira, O. N. Jr. *Langmuir* **2009**, *25*, 3057−3061.
(6) Schmidt, T. F.; Caseli, L.; Viitala, T.; Oliveira, O. N. Jr. *Biochim. Biophys. Acta, Biomembr.* **2008**, *1778*, 2291−2297.
(7) Goto, T. E.; Lopez, R. F.; Oliveira, O. N. Jr.; Caseli, L. *Langmuir* **2010**, *26*, 11135−11139.
(8) He, Q.; Li, J. *Adv. Colloid Interface Sci.* **2007**, *131*, 91−98.
(9) Pavinatto, F. J.; Fernandes, E. G. R.; Alessio, P.; Constantino, C. J. L.; de Saja, J. A.; Zucolotto, V.; Apetrei, C.; Oliveira, O. N. Jr.; Rodriguez-Mendez, M. L. *J. Mater. Chem.* **2011**, *13*, 4995−5003.
(10) Monteiro, D. S.; Nobre, T. M.; Zaniquelli, M. E. D. *J. Phys. Chem. B* **2011**, *115*, 4801−4909.
(11) Dhawan, G.; Sumana, G.; Malhotra, B. D. *Biochem. Eng. J.* **2009**, *44*, 42−52.
(12) Gidalevitz, D.; Huang, Z; Rice, S. A. *Proc. Natl. Acad. Sci. U.S.A.* **1999**, *96*, 2608−2611.
(13) Arisawa, S.; Arise, T.; Yamamoto, R. *Thin Solid Films* **1992**, *209*, 259−263.
(14) Caseli, L.; Crespilho, F. N.; Nobre, T. M.; Zaniquelli, M. E. D.; Zucolotto, V.; Oliveira, O. N. Jr. *J. Colloid Interface Sci.* **2008**, *319*, 100−108.
(15) Katz, E.; Willner, I. *ChemPhysChem* **2004**, *5*, 1085−1104.
(16) Kim, S. N.; Rusling, J. F.; Papadimitrakopoulos, F. *Adv. Mater.* **2007**, *19*, 3214−3228.
(17) Willner, I.; Willner, B. *Nano Lett.* **2010**, *10*, 3805−3815.
(18) Siqueira, J. R. Jr.; Caseli, L.; Crespilho, F. N.; Zucolotto, V.; Oliveira, O. N. Jr. *Biosens. Bioelectron.* **2010**, *25*, 1254−1263.
(19) Kim, J.; Lee, S. W.; Hammond, P. T.; Shao-Horn, Y. *Chem. Mater.* **2009**, *21*, 2993−3001.
(20) Lee, S. W.; Kim, J.; Chen, S.; Hammond, P. T.; Shao-Horn, Y. *ACS Nano* **2010**, *4*, 3889−3896.
(21) Lee, S. W.; Kim, B. S.; Chen, S.; Shao-Horn, Y.; Hammond, P. T. *J. Am. Chem. Soc.* **2009**, *131*, 671−679.
(22) Siqueira, J. R. Jr.; Gasparotto, L. H. S.; Oliveira, O. N. Jr.; Zucolotto, V. *J. Phys. Chem. C* **2008**, *112*, 9050−9055.
(23) Siqueira, J. R. Jr.; Abouzar, M. H.; Bäcker, M.; Zucolotto, V.; Poghossian, A.; Oliveira, O. N. Jr.; Schöning, M. J. *Phys. Status Solidi A* **2009**, *206*, 462−467.
(24) Siqueira, J. R. Jr.; Abouzar, M. H.; Poghossian, A.; Zucolotto, V.; Oliveira, O. N. Jr.; Schöning, M. J. *Biosens. Bioelectron.* **2009**, *25*, 497−501.
(25) Siqueira, J. R. Jr.; Werner, C. F.; Bäcker, M.; Poghossian, A.; Zucolotto, V.; Oliveira, O. N. Jr.; Schöning, M. J. *J. Phys. Chem. C* **2009**, *113*, 14765−14770.
(26) Siqueira, J. R. Jr.; Bäcker, M.; Poghossian, A.; Zucolotto, V.; Oliveira Junior, O. N.; Schöning, M. J. *Phys. Status Solidi A* **2010**, *207*, 781−786.
(27) Siqueira, J. R. Jr.; Maki, R. M.; Paulovich, F. V.; Werner, C. F.; Poghossian, A.; de Oliveira, M. C. F.; Zucolotto, V.; Oliveira, O. N. Jr.; Schöning, M. J. *Anal. Chem.* **2010**, *82*, 61−65.
(28) Caseli, L.; Vinhado, F. S.; Iamamoto, Y.; Zaniquelli, M. E. D. *Colloid Surf., A* **2003**, *229*, 169−180.
(29) Maget-Dana, R. *Biochim. Biophys. Acta, Biomembr.* **1999**, *1462*, 109−140.
(30) Ahuja, R. C.; Caruso, P. L.; Mobius, D. *Langmuir* **1993**, *9*, 1534−1544.
(31) Takahashi, H.; Murase, Y.; Kurihara, K.; Hatta, I.; Arakawa, E.; Takeshita, K.; Matsushita, T. *Jpn. J. Appl. Phys.* **1996**, *35*, L1092−L1095.
(32) Levin, I. W. *Biochemistry* **1985**, *24*, 6282−6286.
(33) Ganim, Z.; Chung, H. S.; Smith, A. W.; deFlores, L. P.; Jones, K. C.; Tokmakoff, A. *Acc. Chem. Res.* **2008**, *41*, 432−441.
(34) Ulrich, W. P.; Voegel, H. *Biophys. J.* **1999**, *76*, 1639−1647.
(35) Jabri, E.; Car, M. B.; Hausinger, R. P.; Karplus, P. A. *Science* **1995**, *268*, 998−1004.
(36) Pandey, R. R.; Saini, K. K.; Dhayal, M. *J. Biosens. Bioelectron.* **2010**, *1*, 1−4.
(37) Dousseau, F.; Pézolet, M. *Biochemistry* **1990**, *29*, 8771−8779.
(38) Pavinatto, F. J.; Caseli, L; Pavinatto, A.; Santos, D. S.; Nobre, T. M.; Zaniquelli, M. E. D.; Silva, H. S.; Miranda, P. B.; Oliveira, O. N. Jr. *Langmuir* **2007**, *23*, 7666−7671.
(39) Gasparotto, L. H. S.; Zucolotto, V.; Oliveira, O. N. Jr.; Siqueira, J. R. Jr. *Electrochem. Solid-State Lett.* **2011**, *14*, P21−P23.